Clim. Past Discuss., doi:10.5194/cp-2016-102, 2016
Manuscript under review for journal Clim. Past
Published: 1 November 2016

Climate of the Past Discussions

Centennial to millennial climate variability in the far northwestern Pacific (off Kamchatka) and its linkage to East Asian monsoon and North Atlantic from the Last Glacial Maximum to the Early Holocene

Sergey A. Gorbarenko [1], Xuefa Shi [2], Min-Te Chen [3], Galina Yu. Malakhova , [4], Aleksandr A. Bosin [1], Yanguang Liu [2], Jianjun Zou [2]

[1] V.I. Il'ichev Pacific Oceanological Institute, Russia

[2] First Institute of Oceanography, SOA, China

[3] National Taiwan Ocean University

[4] North-East Interdisciplinary Science Research Institute FEB RAS, Russia

Abstract

High resolution reconstructions based on productivity proxies and magnetic properties measured from sediment core 41-2 (off Kamchatka), reveal prevailing centennial -millennial productivity/climate variability in the northwestern (NW) Pacific from the Last Glacial Maximum (LGM) to the Early Holocene (EH). The core age model is established by AMS ^{14}C dating using foraminifer shells from the core and by correlating the productivity cycles and relative paleomagnetic intensity records with those of well-dated nearby core, SO-201-12KL. Our results show a pronounced feature of centennial - millennial productivity/climate cycles of the NW Pacific had occurred synchronicity with the summer

Clim. Past Discuss., doi:10.5194/cp-2016-102, 2016
Manuscript under review for journal Clim. Past
Published: 1 November 2016

East Asian Monsoon (EAM) at sub-interstadial scale during the LGM (3 cycles), Heinrich Event 1(3 cycles), and Bølling/Allerød warming (4 cycles), and over the EH (3 cycles). Our comparison of the centennial-millennial variability to the Antarctic EDML (EPICA Dronning Maud Land) ice core suggests a "push" effect of Southern hemisphere temperature gradients on the summer EAM intensifications. Besides the linkages of NW Pacific high productivity and summer EAM, we observed that five low productivity cycles during EH are nearly synchronous with cooling in Greenland, weakening of the summer EAM, and decreases in solar irradiance. We propose that such centennial-millennial productivity/climate variability in the NW Pacific and sequence of sub-stadial/interstadials in the EAM from the LGM to EH are a persistent regional features, synchronous with the Greenland/North Atlantic short-term changes. We speculate that such climate synchronicity was forced also by changes in Atlantic meridional overturning circulation coupled with Intertropical Convergence Zone shifting and the northern westerly jets reorganization.

1. Introduction

Model simulations and proxy-based interpretations led to contradictory results concerning the millennial environmental variability in the northwestern (NW) Pacific and its underlying mechanisms during the last deglaciation. These model and proxy studies suggested either in-phase relationships of deglacial variability between the North (N) Atlantic and NW Pacific (Caissie et al., 2010; Chikamoto et al., 2012; Kienast and McKay, 2001; Seki et al., 2002) or out-of-phase responses (Gebhardt et al., 2008; Okazaki et al., 2010; Sarnthein et al., 2006). The in-phase relationship has been attributed to rapid atmospheric teleconnection in the N hemisphere on years to decadal time scales (Max et al., 2012). The out-of-phase response, however, was proposed to be driven by a seesaw mechanism, with oceanic readjustments between the Atlantic meridional overturning circulation (AMOC) and Pacific meridional overturning circulation. Recent studies on high-resolution and precisely-dated sediment cores from the subarctic NW Pacific, the Sea of Okhotsk, and the western Bering Sea show a deglacial sea surface temperature (SST) evolution similar to the northeastern (NE) Pacific and to the N Atlantic and Greenland temperature variability(Max et al., 2012). The studies suggest a close linkage to deglacial variations in AMOC associated with rapid atmospheric teleconnection, which were responsible for a quasi-synchronous SST development between the N Atlantic and N Pacific during the last deglaciation. On the basis of high resolution X-ray fluorescence (XRF) and sediment surface color reflectance studies on western Bering Sea cores (Riethdorf et al., 2013) a close linkage between millennial-scale productivity changes to the Dansgaard–Oeschger variability were registered in the North Greenland Ice Core Project (NGRIP) ice core, which had been interpreted to support the atmospheric coupling mechanism. A study comparing the subarctic N Pacific dust record to dust content in the NGRIP ice core also shows synchronicity of the timing of abrupt millennial changes during the last 27 ka (Serno et al., 2015). Though a recent study by Praetorius and Mix (2014) based on multidecadal-resolution foraminiferal oxygen isotope records from the Gulf of Alaska reveals a synchronicity of rapid climate shifts between the N Atlantic/Greenland (NGRIP core record) and the NE Pacific between 15.5 to 11 ka, inverse relationships between the Atlantic/Pacific during the Holocene and Heinrich Event (HE) 1 are suggested, while the short-term variability is either not sufficiently resolved or decoupled.

All the instances indicate that a lack of high resolution proxy records in the NW Pacific prohibits precise assessments of any possible climatic teleconnection mechanisms across the basins. Although abrupt centennial-millennial precipitation anomalies over the Last Glacial Maximum (LGM) to the Holocene have been reported in cave sediment $\delta^{18}O$ records of the East Asian monsoon (EAM) (Dykoski et al., 2005; Wang et al., 2001, 2005, 2008; Yuan et al., 2004), the timing and the trend of variability of Early Holocene (EH) regional climate changes are still controversial. In particular, though the EH climate has started from a strong warming in most cases, a Hani peat $\delta^{18}O$ record from northeastern China instead suggest cooling events which are primarily superimposed on a Holocene long-term warming trend (Hong et al., 2009).

Here we present the high resolution results of a suite of productivity proxies, magnetic properties, and lithological changes from the NW Pacific sediment core LV 63-41-2 (hereafter, 41-2) (off Kamchatka) that reveal a sequence of centennial-millennial climate/productivity variability over 20 ka to 8 ka. An age model of this core was constructed by AMS ^{14}C dating and then fine-tuned by correlating the productivity and relative paleomagnetic intensity variability with one well-dated nearby core, SO-201-12KL (hereafter, 12KL) (Max et al., 2012, 2014). With our methodologically robust age controls, we are able to infer a tight linkage between the centennial-millennial productivity variability in the NW Pacific and the sub-interstadial summer EAM intensifications expressed in cave sediment $\delta^{18}O$ records. Our results have enabled us to investigate further any mechanisms controlling the phase relationships of the centennial-millennial variability in the NW Pacific/EAM with those underlying the Greenland/N Atlantic and Antarctic climate changes during the LGM – HE 1 – Bølling/Allerød (B/A) – Younger Dryas (YD) – EH (~20-8 ka).

Clim. Past Discuss., doi:10.5194/cp-2016-102, 2016
Manuscript under review for journal Clim. Past
Published: 1 November 2016

Climate of the Past Discussions

2 Materials and methods

2.1 Coarse fraction measurement

Sediment core 41-2 was recovered in the NW Pacific off Kamchatka peninsula (water depth 1924 m; 52°34,' N; 160°00,6' E; core length 467 cm) during joint Russian-Chinese expedition in 2013. Weight percentage of coarse fraction (CF) >63 μm and <2000 μm, sampled every 1 cm and separated by sieve washing, was calculated as ratios of CF weight to the weight of the dry bulk sediment. The CF of sediments, indicator of the component of materials mainly transported to the study region by sea ice (Gorbarenko et al., 2003; Lisitzin, 2002; Sakamoto et al., 2005), is used as an ice rafted debris (IRD) proxy here. The tephra material input in the CF was estimated by semi-quantitative component analyses of this fraction with a total of 12 ranged scales. We made estimations of various components including terrigenous and volcanogenous particles, benthic and planktonic foraminifera, diatom frustules, and radiolarians in this study.

2.2 Chlorin content measurement

The chlorin content of core 41-2 was measured on samples taken every 1 cm and on core 12KL every 2 cm through the whole cores using a Shimadzu UV-1650PC spectrophotometer according to the modified method of Harris et al. (1996).

Clim. Past Discuss., doi:10.5194/cp-2016-102, 2016
Manuscript under review for journal Clim. Past
Published: 1 November 2016

2.3 Total organic carbon (TOC), calcium carbonate, and color b* measurements

Total carbon content and inorganic carbon in core 41-2 were measured every 2 cm through the core depth by coulometry using an AN-7529 analyzer (Gorbarenko et al., 1998). TOC content was determined by computing the difference between total carbon and inorganic carbon content. A color b* index (psychometric yellow–blue chromaticness) was measured using a Minolta CM-2002 color reflectance spectrophotometer that generates visible-light reflectance data (400 to 700 nm wavelengths) (Harada, 2006) of the core every 1cm. In this study we used the trend of color b* that well correlates with the changes in biogenic opal contents in sediment cores (Nürnberg and Tiedemann, 2004).

2.4 Radiocarbon dating (AMS ^{14}C)

AMS ^{14}C-ages were measured on monospecific samples of the planktic foraminifers *Neogloboquadrina pachyderma* sinistral (*N. pachyderma* sin.) from a 125–250 μm fraction and benthic foraminifera *Epistominella pacifica*, and *Uvigerina parvocostata* from the 250–350μm fraction of the core. The radiocarbon dating has been performed by the Dr. John Southon at the Keck Carbon Cycle AMS Facility (UCIAMS) in the Earth System Science Department of the University of California, USA. The same reservoir age (900 ± 250 yr) of the NW Pacific surface water (Max et al., 2012) was adopted in this study to calibrate the ^{14}C ages of our samples into calendar ages for establishing consistent AMS ^{14}C chronologies of cores 41-2 and 12KL. When using benthic foraminifera for AMS ^{14}C dating on our cores, we take the age difference of 1400 yrs between coexisting benthic and planktic foraminifera ages to make further corrections (Max et al., 2014). All reservoir age corrected ^{14}C data were converted into calendar age by using Calib Rev 6.0 (Stuiver and Reimer, 1993) with the IntCal09 and Marine09 data sets (Reimer et al., 2009).

2.5 Magnetic property measurements

Magnetic property analyses of cores 41-2 and 12KL were conducted by taking samples every 2.4 cm throughout the cores. Volume magnetic susceptibility (MS) of these samples was measured using an AGICO MFK1-FA device. The characteristic remnant magnetization (ChRM) of the cube samples was measured in the same way by studying the stability of natural remanent magnetization (NRM) in the alternative magnetic fields of up to 80-100 mT on the basis of analysis of Zijderveld vector plots, using an AGICO LDA-3A device and rock-generator AGICO JR-5a (Zijderveld, 1964). The module and direction of NRM were measured on a JR-5A rock-generator after the stepwise demagnetization of reference samples by alternating magnetic fields with a vanishing amplitude (Malakhov et al., 2009). Ahysteretic remanent magnetization (ARM) was generated using an AGICO AMU-1A device and measured by the JR-5A rock-generator. Relative paleomagnetic intensity (RPI) of the studied core sediments was determined by the normalization of the ChRM after demagnetization at 20 mT by ARM (ChRM/ARM) (Tauxe, 1993). The sediment paramagnetic magnetization (PM) was measured for each sample from curves of magnetic hysteresis by a J Meter coercitive spectrometer at Kazan State University, Kazan, Russia (Enkin et al., 2007; Jasonov et al., 1998). PM was formed in marine sediments of silicate, paramagnetic iron sulphide (FeS), and fine clay minerals transported from land as an eolian dust through atmosphere circulation by westerly jets. Therefore, the sediment PM may serve as a proxy of the land aridity and/or atmosphere circulation pattern changes in response to climate changes.

2.6 XRF measurements

Core 41-2 elemental composition, given in peak area (counts per second, cps), were measured at 0.5 cm resolution using the Itrax XRF core scanner at the First Institute of Oceanography, State Oceanic Administration, China. The Itrax XRF core scanner was set at 20 s count times, 30 kV X-ray voltage, and an X-ray current of 20 mA. Though absolute elemental concentrations are not directly available from the micro-XRF measurements, the count values can be used as estimates of the relative concentrations. The count values may be influenced by the changes in the physical properties of the sediment, such as the surface roughness of the core (Röhl and Abrams, 2000). However, the grain size of the 41-2 core is rather fine and the surface has been processed to be as flat as possible to minimize any effects from changing physical properties or roughness during the scanning.

In this study, we paid attention to the scanning results for estimating biogenic Ba, Br and Si (Ba-bio, Br-bio and Si-bio respectively) contents in our sediment cores, which serve as proxies of productivity. The content of Ba-bio was estimated by subtraction of its terrigenous component (Ba-ter) from the total bulk Ba concentration in sediment (Ba-tot). The terrigenous component, in turn, was calculated from empirical regional $(Ba/Al)_{ter}$ ratios in the sediment core with the lowest Ba-tot contents:

$$\text{Ba-bio} = \text{Ba-tot} - (\text{Ba/Al})_{ter} * \text{Al}$$ (by Goldberg et al. (2005)).

Br-bio and Si-bio were calculated using the same technique.

Clim. Past Discuss., doi:10.5194/cp-2016-102, 2016
Manuscript under review for journal Clim. Past
Published: 1 November 2016

3. Results

AMS radiocarbon data for core 41-2 are presented in Table 1. The sediment PM and MS, and a suite of productivity proxies - TOC, chlorin, $CaCO_3$, Ba-bio, Br-bio, Si-bio contents, and color parameter b* with four AMS ^{14}C data are presented for core 41-2 versus depth (Fig. 2). We observed high productivity in the middle part of the core (interval ~315-230 cm), which could be chronologically assigned to the B/A warming right after the termination of the last glaciation (467-315 cm). The high productivity during the B/A warming is a common feature in the far NW Pacific and its marginal seas (Galbraith et al., 2007; Gorbarenko, 1996; Gorbarenko et al., 2005; Gorbarenko and Goldberg, 2005; Keigwin, 1998; Seki et al., 2004). The interval at ~230-190 cm with a decreased trend of productivity is likely associated with the YD cooling. After this low productivity/cold climate event the high productivity/warm trend in the upper 190 cm of the core is presumably related to the Holocene warm climate condition.

Time resolutions for our core 41-2 data over LGM-YD periods are ~30 years for chlorin and color b*, ~60 years for TOC, $CaCO_3$ and magnetic parameters (PM, MS and RPI), and ~15 years for the Ba-bio, Br-bio, Si-bio contents. All the resolutions are high enough to allow us to detect centennial-millennial scale climate variability in the far NW Pacific. Our high resolution productivity and magnetic records presented here reveal nearly synchronous the centennial-millennial cycles associated with abrupt productivity/environmental variability with mechanisms likely similar to established earlier regularities at the orbital-millennial scale (Fig. 2). Therefore, in particular we suggest that the sharp increases shown in our productivity records demonstrate a quick response of the oceanic climate system

Clim. Past Discuss., doi:10.5194/cp-2016-102, 2016
Manuscript under review for journal Clim. Past
Published: 1 November 2016

of the NW Pacific to abrupt global warming and vice versa. In results, our productivity and magnetic records show that 6 short warm events happened during the last glacial and 4 warm events during the B/A warming (Fig. 2). During the EH, our records show 5 short cold events and 3 warm events. We notice that a cold event at depth 117-122 cm with an age of ~9.12 ka (Table 1) is well-correlated with the 9.3 ka cold event in Greenland ice core records (Rasmussen et al., 2014). Moreover, a cold event identified at depth 106-109 cm of our core also links well with the 8.2 ka cold event in Greenland ice cores, a well-known chronostratigraphic marker in the Early to Middle Holocene (Walker et al., 2012).

Our records of the CF percentages, amount of volcanic particles in CF, and MS indicate high IRD values below a 315 cm depth of the core. A significant increase of CF to the top in the upper 220 cm of the core was mostly driven by increased tephra input (Fig. 2). Our MS record also shows higher terrigenous input in the interval of 230-205 cm included in the YD (Fig. 2). A compilation of all our proxies of productivity, PM, and RPI of core 41-2 and a comparison with ones of core 12KL are shown in Fig. 3. The color b* indices and Ca/Ti ratios (analog of $CaCO_3$ content) of core 12KL were extracted from Max et al. (2012, 2014) available on PANGAEA Data Publisher for Earth & Environmental Science (http://dx.doi.org/10.1594/PANGAEA.830222).

4. Age model

An age model of core 41-2 was constructed using all available AMS ^{14}C dating, with more age control points identified by correlating the centennial-millennial events of the productivity proxies, RPI

Clim. Past Discuss., doi:10.5194/cp-2016-102, 2016
Manuscript under review for journal Clim. Past
Published: 1 November 2016

and PM of our core with those of the well-dated nearby core 12KL (Max et al., 2012, 2014) (Fig. 3). The age tuning used in this study assumes a synchronous pattern of productivity, RPI and PM variability in the far NW Pacific since the last glacial. With this framework of age model developments, the centennial-millennial variability of productivity proxies, magnetic parameters earlier identified in core 41-2 are closely matched in the both cores; they show regionally coherent sequences of productivity/environmental cycles (events) from the last glaciation, the B/A warming to the EH (Fig. 3). We noticed that the available for core 12KL the Tiedemann/Max age model (Max et al., 2012, 2014) was based on the AMS ^{14}C data and correlation of color b* index with the NGRIP $\delta^{18}O$ curve (PANGAEA Data Publisher). By adopting this age model of core 41-2, all available AMS ^{14}C dating of core 12KL (with one exception for an age dating of 16.53 ka at depth 695 cm) were transferred successfully to core 41-2 within related productivity cycles and RPI values correlation (Fig. 3). Derived radiocarbon framework of both cores allow us to infer also close correlation of the productivity/environmental cycles identified in the cores with sub-interstadial of absolute U-Th dating $\delta^{18}O$ of calcite recorded in the China caves stalagmites over the 20-8 ka BP (Dykoski et al., 2005; Wang et al., 2008) (Fig. 3), which may be used for further tuning of our age model. In results, the key time points of core 41-2 were based on the available AMS ^{14}C data of core 41-2, depths correlated with core 12KL AMS ^{14}C datum plus correlation of the productivity/environmental cycles with sub-interstadials of the highly resolved, absolutely dated EAM records (Table 2). In the upper part of core we prefer to use correlation with data of core 12KL because of very high sedimentation rate and since they were measured for planktonic foraminifera.

5. Discussion

With the new age controls our productivity proxies and magnetic results of core 41-2, and some of them for core 12KL (Max et al., 2012, 2014) reveal sequence of noticeable centennial-millennial scale events of increased productivity and decreased PM in the far NW Pacific off Kamchatka over the last 21 ka (Fig. 4). As was mentioned these events changes in-phase with sub-interstadials of $\delta^{18}O$ calcite of Chinese stalagmites (CsI) associated with stronger summer EAM (Wang et al., 2008) and, to some extent, are linked to Greenland ice core sub-interstadials (GsI) (North Greenland Ice Core Project members, 2004) (Fig. 4). All the linkages suggest the centennial-millennial productivity changes in the far NW Pacific were likely associated with climatic shifts to warmer and/or higher nutrient conditions in surface water synchronously with CsI of the summer EAM. Our high resolution records show clearly that three centennial-millennial warmer/higher productive (CsI/GsI) events had occurred during the LGM, three CsIs/GsIs during the HE 1, four CsIs/GsIs during the B/A warming, and three CsIs/GsIs during the EH (Fig. 4). Possible mechanisms responsible for the in-phase relationships or the synchronicity of the centennial-millennial scale events between the NW Pacific productivity and summer EAM are discussed and proposed below.

5.1. N-S hemispheres climatic linkages of centennial-millennial climate/environment changes over the LGM - HE 1- B/A warming

Identifying any linkages of centennial–millennial climate changes in the Northern Hemisphere between the NW Pacific, EAM, and N Atlantic/Greenland and the climate changes recorded in Antarctic ice core records from the Southern Hemisphere is important to us, to deepen our understanding of the mechanisms responsible for the timing and spatial propagation patterns that resulted from the abrupt variability in the global climate and environmental system. In order to test the linkages, we demonstrate here the correlation among the highly resolved U-Th dated $\delta^{18}O$ records of the composite Hulu and Dongge caves sediments (Dykoski et al., 2005; Wang et al., 2008), the ~20-year averaged resolution $\delta^{18}O$ and Ca^{2+} content records of the GISP2 and NGRIP with 5 point running mean on the annual-layer counted GICC05 age scale (Rasmussen et al., 2014), and the $\delta^{18}O$ record of the EPICA Dronning Maud Land (EDML) ice core from Antarctica (EPICA Community Members, 2006) on the methane synchronized timescale with the NGRIP core over the past 25 ka (Fig. 5). The Ca^{2+} content in the Greenland ice cores serves as a proxy for dust content governed by atmosphere circulation changes. It has been suggested that the nearly synchronous ice core $\delta^{18}O$ and Ca^{2+} changes reflect the shifting of Greenland atmospheric dust loading and is closely linked to the atmospheric circulation and climate changes in the high-latitude of N hemisphere. Initially the persistent millennial scale changes shown in the Greenland ice core records were defined as interstadials (GI) and stadial (GS) (Johnsen et al., 1992), but have been refined by INTIMATE event stratigraphy studies which introduced the subdivision of the GI-1 into sub-interstadials GI-1a to GI-1e. Furthermore, the GS-2.1 was subdivided into sub-Stadial GS-2.1a (over the HE 1), GS-2.1b (LGM), and GS-2.1c (Björck et al., 1998; Rasmussen et al., 2014) (Fig. 5). It also has been noted that the some $\delta^{18}O$ differences in coeval $\delta^{18}O$ values between Summit and NGRIP ice cores over the LGM period, and abrupt millennial scale

Clim. Past Discuss., doi:10.5194/cp-2016-102, 2016
Manuscript under review for journal Clim. Past
Published: 1 November 2016

variations, were likely governed by changes in the N American Ice Sheet volume and N Atlantic sea-ice extent, that result in the changes of meridional gradients in the $\delta^{18}O$ of Greenland ice (Seierstad et al., 2014).

On the basis of the high-resolution NGRIP core investigation (less one year) over 15-11 ka, Steffensen et al. (2008) have suggested that at the beginning of the GI, the initial northern shift of the Intertropical Convergence Zone (ITCZ), identified in a sharp decrease of dust within a 1-3 year interval, triggered an abrupt shift of Northern Hemisphere atmospheric circulation. The circulation pattern changes forced a more gradual change (over 50 years) of the Greenland air temperature associated with high latitude atmosphere circulation and westerly jets ways reorganization. Evidence from a loess grain size record in NW Chinese Loess Plateau (Sun et al., 2011), infer the linkage of the changes in EAM strength and Greenland temperature over the past 60 ka, and suggests a common force driving both changes (Sun et al., 2011). Using a coupled climate model simulation, Sun et al. (2011) investigated the effect of a slow-down of AMOC on the monsoon system and found a stronger winter EAM that supplies more dust to the Loess Plateau with a reduction in summer monsoon precipitation over East Asia. This study indicates that AMOC is a driver of abrupt change in EAM, with the northern westerlies as the transmitting mechanism from the N Atlantic to the Asian monsoon regions. Other evidences of teleconnection between the EAM and N Atlantic on a millennial timescale come from the investigation of the Japan Sea sediments. Nagashima et al. (2011) infer that temporal changes in the provenance of eolian dust in Japan Sea sediments reflect changes in the westerly jet path over East Asia, happened in phase with Dansgaard-Oeschger cycles.

EPICA community members (2006) show that methane synchronization of the EDML and the NGRIP $\delta^{18}O$ records reveal one-to-one alignment of each Antarctic warming with a corresponding stadial in Greenland ice cores, implying a mechanism of bipolar seesaw on these time scales. Changes in the heat and freshwater flux were connected to the AMOC and a stronger AMOC leads to increased transport of heat from the Southern Ocean heat reservoir. EAM studies (Wang et al., 2001) have suggested that between 11,000 and 30,000 yr BP the Chinese interstadials (CI) recorded in $\delta^{18}O$ calcite of cave stalagmites had happened apparently synchronously with the GIs and therefore CIs were likely related to Antarctica cold events also. For example, smoothed warmer condition in the Antarctic at 23.6-24.2 ka was synchronous with abrupt climate cooling and increases in dust content in the Greenland ice cores NGRIP and GISP2, coeval to HE 2 of the N Atlantic and in-phase with summer EAM weakening (GS/CS-3.1) (Fig. 5). Subsequent Antarctica cooling since 23.4 ka was accompanied by Greenland warming with two sharp interstadials GI-2.2 and GI-2.1 with nomenclature of Rasmussen et al. (2014) and China interstadial CI2 coeval with summer EAM intensification – sub-interstadial CsI-2.9 (Fig. 5).

The uncertainties in the chronologies of the Greenland and Antarctica temperature and EAM records is very small (<2 %) thus suggest their tight relationship during the last 25ka (Fig. 5). Cross correlation of the EAM intensity and Greenland climate variability calculated by correlation of $\delta^{18}O$ values between the calcite of Chinese stalagmites responsible for EAM variability (Wang et al., 2008) and NGRIP and GISP 2 ice cores responsible for the Greenland climate (Rasmussen et al., 2014) by moving windows at 1000, 2000 and 3000 years show their significant synchronization (positive correlation) during period of 16.5-9.0 ka BP (Fig. 6). The cross correlation of the EAM and the

Clim. Past Discuss., doi:10.5194/cp-2016-102, 2016
Manuscript under review for journal Clim. Past
Published: 1 November 2016

Greenland NGRIP ice core during earlier (25-16.5 ka ago) and later (9-1 ka ago) periods demonstrates absence of significant correlation (within ranging at ±0.25), or occurrence of weak synchronization (positive correlation) (Fig. 6). The statistics imply that the seesaw mechanism between the EAM/NW Pacific and the Greenland/N Atlantic during 25-1 ka is not effective, however being in line with empiric results of the EAM and the Greenland teleconnection by shifting of the westerly jet path (Nagashima et al., 2011; Sun et al., 2011).

It also has been suggested that a monsoon intensity index including the EAM was controlled not only by Northern Hemisphere temperature (‘pull’ on the monsoon, which is more intense during boreal warm periods), but also by the pole-to-equator temperature gradient in the Southern Hemisphere (‘push’ on the monsoon which is more intense during cold periods) that leads to enhanced boreal summer monsoon intensity and its northward propagation (Rohling et al., 2009; Rossignol-Strick, 1985; Xue et al., 2004). Since the summer EAM transports heat and moisture from the West Pacific Warm Pool (WPWP) across the equator and to higher northern latitudes (Wang et al., 2001), the temperature gradient in the Southern Hemisphere “pushes” the summer EAM intensity by means of its influence on the latitudinal/longitudinal migrations or expansion/contraction of the WPWP. This also explains the different form of responses of EAM and Greenland interstadials and sub-interstadials, because the migration of the WPWP may have responded much more slowly than the atmosphere. All the above interpretations are consistent with observed here, that the variability in the δ^{18}O record of Chinese EAM changes was more gradual then in the δ^{18}O of Greenland ice cores, and the amplitude changes of the EAM are more similar to the Antarctic air temperature changes (Fig. 5).

With the same subdivision as in Greenland records, the EAM sub-interstadials (CsI)/NW Pacific centennial-millennial productivity/environment cycles were put on the N-S hemispheres climate variability with three CsIs identified from the interval of 25-20 ka (Fig. 5). Moreover, we found three EAM/NW Pacific sub-interstadials within GS-2.1a (namely CsI 2.1, CsI 2.2 and CsI 2.3), four CsIs in GS-2.1b (CsI 2.4 to CsI 2.7), and two in GS-2.1c (CsI 2.8 and CsI 2.9) (Fig. 5). During B/A warming when Antarctic temperature was decreased, four EAM sub-interstadials (CsI-1a–CsI-1e) have varied in-phase with Greenland sub-interstadials (Björck et al., 1998).

Our results derived from two studied cores indicate tight in-phase linkages between the far NW Pacific centennial-millennial productivity/environment cycles and the summer EAM intensity sub-interstadials variability (Fig. 4) over GS-2.1–GI-1. These evidence leads us to suggest that the centennial-millennial changes in the NW Pacific and EAM have been forced by similar/or may be less pronounced mechanisms as for interstadials by the shifting of the ITCZ with reorganization of the N Hemisphere atmospheric circulation and the northern westerly jets. Though the responses of the EAM sub-interstadials are more smoothly compared with Greenland ones (Fig. 5), the most of them had occurred synchronicity with ones of the Greenland NGRIP ice core and out of phase with ones of the Antarctica record (Fig. 5). Thus we infer that revealed for studied cores centennial-millennial productivity/environment cycles over 20-8 ka ago are persistent peculiarities of the productivity/environment variability of the NW Pacific couples with EAM sub-interstadials changes which may be used as template in the regional high resolution paleoceanography and sediment stratigraphy. Four productivity/environment events in the far NW Pacific during the B/A warming had occurred in-phase with the EAM and Greenland temperature sub-interstadials (Figs. 4 and 5). Recent

Clim. Past Discuss., doi:10.5194/cp-2016-102, 2016
Manuscript under review for journal Clim. Past
Published: 1 November 2016

high-resolution investigations on Bering Sea sediment cores from the "Bering Green Belt" (Kuehn et al., 2014) have documented four well-dated laminated sediment layers during the B/A warming-beginning of Holocene, with one from them for the Preboreal. The synchronicity of Bering Sea laminated sediment layers with the Greenland sub-interstadial during B/A warming provides one more piece of evidence supporting the close atmospheric teleconnection between the N Pacific, the EAM, and the N Atlantic.

5.2 NW Pacific productivity trends over the LGM- HE 1

Beside of the centennial -millennial productivity/environmental cycles, we find common NW Pacific productivity trends over the LGM and Heinrich E 1 with some differences in other types of productivity proxies. According to the sharp increase of Antarctica temperature, dust content in the Greenland ice cores and significant decrease in the summer EAM we put boundary of LGM/HE 1 on nearly the 17.8 ka ago (Fig. 5). This age is a little earlier to that being placed at ~17.5 ka which is a timing for the beginning of catastrophic iceberg discharges in the HE 1, but nearly coincides with the abrupt increase of the $^{231}Pa/^{230}Th$ ratio in the N Atlantic core OCE326-GGC5, which marks the beginning of the collapse of AMOC (McManus et al., 2004).

During the LGM most productivity proxies demonstrate minimum primary production in the far NW Pacific without definite trends although the Si-bio of core 41-2 and color b* of core 12KL show even small negative trend versus time (Fig. 4). Severe environmental condition in the central Asia inferred from vegetation reconstruction (Bezrukova et al., 2011) (Fig. 5) promote to increase in cold season sea ice covering and high IRD accumulation in studied region (Fig. 4) that hamper productivity. It is consistent with early established minimum of productivity in the NW Pacific due to strong stratification prevented nutrients supply for supporting productivity in surface waters (Gebhardt et al., 2008).

Since 17.8 up to 15.5 ka, the core 41-2 productivity proxies such as Ba-bio, Br-bio, TOC and chlorin, associated with production of calcareous phytoplankton (mostly coccolithophores), show significant increased trends simultaneous to gradual Antarctic warming accompanied by strongly diminished of AMOC (McManus et al., 2004). The patterns are consistent with the see-saw N-S hemispheres mechanism (Broecker, 1998). The diminished AMOC resulted in a major cooling of the N Atlantic surface water and, most likely, reduced water evaporation in the N Atlantic and therefore Atlantic–Pacific moisture transport. This condition facilitates a reduction of precipitation and hence an overall increase of surface water salinity and decrease of surface stratification in the N Pacific. Moreover, this condition promotes an intensification of the intermediate water ventilation in the N Pacific and also nutrient supply into euphotic layer. The observed trends of our productivity proxies are in concord with strong intensification of the intermediate depth water ventilation in the N Pacific during HE 1 (Max et al., 2014) based on the $\delta^{13}C$ foraminifera data from the intermediate water and radiocarbon-derived ventilation ages. However, rather constant $CaCO_3$ values in both cores (water depth 1924-2145 m) during LGM-HE 1 do not indicate the changes of the water ventilation at these depths in the N Pacific over that time span because carbonate concentration in the sediment strongly defined by the ventilation (Yu et al., 2014). While the productivity proxies Si-bio and color b*, associated with siliceous phytoplankton production (mostly diatoms), do not show significant trends since HE 1 to ~15.5 ka. The strong sea ice effect indicated by our CF and MS records (Figs. 2; 4) was more significant in our studied area and likely overwhelm the productions of diatom algae for coccolithophores due to a large spring-early summer surface water stratification during seasonal sea ice melting.

A sharp increase of NW Pacific primary production since ~15.5 ka was indicated by most our productivity proxies which culminated by strong productivity peak of sub-interstadial GI-1e at beginning of the B/A warming (Fig. 4). Synchronous decrease of sea ice influence in the studied region since ~15.5 ka marked by dropping in the CF and MS was favor for decrease of surface stratification the rise of diatom production as indicated by the sharp increases of Si-bio and color b* (Figs. 4 and 2). The timing of decrease in the sea ice cover since ~15.5 ka is consistent with the surface ocean warming (Max et al., 2012) and also consistent with the central Asia vegetation/environment amelioration inferred by Bezrukova et al. (2011) by pollen reconstructions (Fig. 5). Such pattern of the productivity changes in the N Pacific and the Bering Sea during glacial/interglacial transition was observed in other cores (Caissie et al., 2010; Galbraith et al., 2007; Gebhardt et al., 2008; Keigwin, 1998) and was, likely, a persistent feature for the N Pacific and its realm forced by resumption of the AMOC at the B/A beginning coeval with the cooling in the Antarctica (Fig. 5). In the Okhotsk Sea, being strongly intruded in the NE Asia continent, the beginning of the diatom production and accumulation of the diatomaceous sediments had occurred only since the Middle Holocene (5-6 ka BP) due to the later diminish of sea-ice cover and later breakdown of spring/early summer surface water stratification compared with ones of the far NW Pacific (Gorbarenko et al., 2014).

Clim. Past Discuss., doi:10.5194/cp-2016-102, 2016
Manuscript under review for journal Clim. Past
Published: 1 November 2016

5.3 The EH

During EH our records demonstrate a series of abrupt cold Chinese sub-stadials (CsS) and warm CsIs that are well-correlated with variability shown in Dongge and Hulu caves $\delta^{18}O$ records (Dykoski et al., 2005; Wang et al., 2008), and $\delta^{18}O$ records of Greenland ice cores: CsS1 (~8.2ka), CsS2 (~9.2ka), CsI1, CsS3 (~10.2ka), CsI2, CsS4 (~10.9ka), CsS4' (~11.1ka), and CsI3 (Fig. 4). These sub-stadials and sub-interstadial were also put on the N-S hemisphere climate variability patterns (Fig. 5). Visual comparison with the EAM and Greenland ice cores records show synchronicity (positive correlation) of the warmer climate/increased productivity events in the NW Pacific with the Greenland abrupt warmer climate cycles and summer EAM intensity events and vice versa over the EH as well (Figs. 4 and 5). Pollen reconstructed dated variability of the climate/environment conditions of the southeastern Siberia (Lake Kotokel, Lake Baikal region) (Bezrukova et al., 2011) demonstrated nearly the same type of the centennial-millennial climate variability patterns that shows positive climate linkages with climate in the North Hemisphere (N Atlantic, NW Pacific, EAM) over the EH (Fig. 5). Well-dated high resolution lithological and geochemical results from the Yanchi playa (NE China) clearly show a separation of three sharp cooling events at 8.2 ka, 9.9-10.1ka, and 11.0-11.2 ka, synchronous with the cooling shown in the Greenland ice core records (Yu et al., 2006). Yu et al. (2006) explain that correlation by linkages of the tropical Pacific and the N Atlantic. Moreover, high resolution geochemical and lithological analyses of the Arolik Lake sediments (southwestern Alaska) provide evidence that centennial-scale

Clim. Past Discuss., doi:10.5194/cp-2016-102, 2016
Manuscript under review for journal Clim. Past
Published: 1 November 2016

climate shifts during the Holocene were similar between the subpolar regions of the N Atlantic and N Pacific (Hu et al., 2003).

These regional climate shifts had occurred coherent with the periodicities of solar activity and production of the cosmogenic nuclides ^{14}C and ^{10}Be. The production rates of these cosmogenic nuclides are negatively correlated with total solar irradiance through the strength of magnetic fields embedded into solar winds speed. Small variations in solar irradiance could be responsible for pronounced changes in northern high-latitude environments (Hu et al., 2003). Our records of the centennial-millennial warmer climate/ increased productivity cycles in the far NW Pacific are simultaneous with the sharp variability in the EAM and the Greenland temperature over the EH and in-phase, within the uncertainty of our age controls, with the decreased production of nuclide ^{14}C and therefore with increased solar input and vice versa (Fig. 5). Nearly synchronicity in the changes of the centennial-millennial productivity and magnetic proxies obtained in the two studied cores with the $\delta^{18}O$ records of Chinese cave sediments, the Greenland ice cores, and with the nuclide ^{14}C production during the EH (Figs. 4, 5) imply that variability of the NW Pacific climate and environmental condition has been tightly related with EAM and N Atlantic/Greenland climate changes by atmospheric coupling mechanisms over the studied period of 20-8 ka. In summary, our analysis indicates a tight linkage and coherent, persistent pattern of the centennial-millennial scale climate changes in the N Hemisphere over the LGM-EH which may be serve as template in high resolution climate variabilities and sediment stratigraphy of the moderate-high latitudes.

6. Conclusion

This study presents high resolution records of a suite of productivity proxies TOC, $CaCO_3$, chlorin, color b*, Ba-bio, Br-bio, Si-bio and content of CF, MS, PM and RPI from a sediment core 41-2 taken from the NW Pacific (East Kamchatka slope). Our results indicate a sequence of 13 centennial-millennial scale regional productivity increased /environment amelioration events over the LGM-EH in the far NW Pacific.

The age model of core 41-2 was constructed by using available AMS ^{14}C dating, with more age control points identified by correlating the centennial-millennial events of the productivity proxies, RPI and PM of our core with those of the well-dated nearby core 12KL (Max et al., 2012, 2014). Thus all available AMS ^{14}C dating of core 12KL (with one exception for an age dating of 16.53 ka at depth 695 cm) were transferred successfully to core 41-2. Derived radiocarbon framework of both cores allow us to infer also close correlation of the productivity /environmental cycles identified in these cores with sub-interstadial of absolute U-Th dating $\delta^{18}O$ of calcite recorded in the China caves stalagmites over the 20-8 ka BP (Dykoski et al., 2005; Wang et al., 2008), which were used for further fine age model construction. Therefore our records from studied cores show synchronicity of NW Pacific centennial-millennial higher productivity/environment amelioration events with EAM sub-interstadials during 20-8 ka. Three NW Pacific abrupt productivity increase events are tightly linked to CsIs during the LGM (20-17.8 ka), three during HE 1 (17.8-14.7 ka), and four during B/A warming and three over the EH. Our new reconstruction suggests that the NW Pacific centennial-millennial productivity increase/summer EAM intensified events are positively correlate with Greenland warming, indicating a tight atmospheric teleconnection between the N Pacific and the N Atlantic, most likely by ITCZ shifting and reorganization of the northern westerlies and echoes the similar mechanism proposed in previous studies for the N hemisphere interstadials and stadials (Caissie et al., 2010; Kienast and McKay, 2001; Max et al., 2012; Riethdorf et al., 2013). Especially highlighted here is that our comparison to $\delta^{18}O$ records of the EDML ice core and of the Chinese stalagmites on the centennial-millennial time scale over glacial and deglaciation suggests a Southern Hemisphere "push" effect on the boreal summer EAM propagation. The involvement of Southern Hemisphere "push" effects offers better interpretation on what have been responsible for the differences in the observed rate of changes of the EAM and Greenland interstadials and sub-interstadials and a much slower reorganization of the WPWP location or expansion/contraction with their impacts on atmosphere circulation are possibly attributed to the differences too.

During the LGM our results indicate productivity minima that are consistent with previous observations in the NW Pacific, severe vegetation/climate condition in the central Asia (Bezrukova et al., 2011) and therefore strong regional sea ice covering are consistent with the hypothesis that proposes a strong stratification prevented nutrients supply for supporting productivity in surface waters (Gebhardt et al., 2008). The productivity proxies associated with calcareous phytoplankton productions show significant increased trends since 17.8 to 15.5 ka. These trends share the same structure and the rate of changes of the gradual Antarctic warming accompanied by significantly diminished AMOC (McManus et al., 2004). The cooling of the N Atlantic surface water reduced water evaporation in the N Atlantic and Atlantic–Pacific moisture transport, which in turn, facilitates the increased surface water salinity and decreases surface stratification in the N Pacific. The weakening stratification further intensifies the intermediate water ventilation in the N Pacific and nutrients supply into the euphotic layer. Especially noticed is that a sharp increase of NW Pacific primary production since nearly 15.5 ka was indicated by nearly all productivity proxies accompanied by some climate warming and decrease in sea ice covering. Subsequent a strong productivity spike of sub-interstadial GI-1e at beginning of the B/A warming is associated with a resumption of the AMOC and the further decrease of sea ice influence accompanied by rise of diatom production.

The synchronicity in changes of the NW Pacific centennial-millennial productivity events with the $\delta^{18}O$ of Chinese stalagmites calcite, Greenland ice cores and with the nuclide ^{14}C production during the EH (Figs. 4; 5) imply that variability of the NW Pacific climate is tightly linked to summer EAM and N Atlantic/Greenland climate changes. The linkage is likely driven effectively by atmospheric coupling mechanisms forced by solar irradiance variability. Regardless what specific driving mechanisms are responsible for the linkage, the centennial-millennial and sub-stadial/interstadial productivity variability in the NW Pacific and the linkage to EAM from the LGM to EH reported here is a persistent feature of the high resolution far NW Pacific paleoceanography and sediment stratigraphy, synchronous with the Greenland/N Atlantic short-term changes.

Acknowledgements

This research work was supported by the RFBR–Russia Fund of Basic Research – Russia project (13-05-00296a, 16-55-53048 and 16-05-00127), Russian Federation budget No 01201363042, National Natural Science Foundation of China projects (41420104005, 40710069004 and 40431002) and the

Clim. Past Discuss., doi:10.5194/cp-2016-102, 2016
Manuscript under review for journal Clim. Past
Published: 1 November 2016

Russia-Taiwan Research Cooperation project 14-HHC-002. We are appreciated to Dr. John Southon (USA) for AMS 14C dating.

References

Bezrukova, E. V., Tarasov, P. E., Kulagina, N. V., Abzaeva, A. A., Letunova, P. P. and Kostrova, S. S.: Palynological study of Lake Kotokel' bottom sediments (Lake Baikal region), Russ. Geol. Geophys., 52(4), 458–465, doi:10.1016/j.rgg.2011.03.008, 2011.

Björck, S., Walker, M. J. C., Cwynar, L. C., Johnsen, S., Knudsen, K.-L., Lowe, J. J. and Wohlfarth, B.: An event stratigraphy for the Last Termination in the North Atlantic region based on the Greenland ice-core record: a proposal by the INTIMATE group, J. Quat. Sci., 13(4), 283–292, doi:10.1002/(SICI)1099-1417(199807/08)13:4<283::AID-JQS386>3.0.CO;2-A, 1998.

Broecker, W. S.: Paleocean circulation during the Last Deglaciation: A bipolar seesaw?, Paleoceanography, 13(2), 119–121, doi:10.1029/97PA03707, 1998.

Caissie, B. E., Brigham-Grette, J., Lawrence, K. T., Herbert, T. D. and Cook, M. S.: Last Glacial Maximum to Holocene sea surface conditions at Umnak Plateau, Bering Sea, as inferred from diatom, alkenone, and stable isotope records, Paleoceanography, 25(1), PA1206, doi:10.1029/2008PA001671, 2010.

Chikamoto, M. O., Menviel, L., Abe-Ouchi, A., Ohgaito, R., Timmermann, A., Okazaki, Y., Harada, N., Oka, A. and Mouchet, A.: Variability in North Pacific intermediate and deep water ventilation during Heinrich events in two coupled climate models, Deep Sea Res. Part II Top. Stud. Oceanogr., 61–64, 114–126, doi:10.1016/j.dsr2.2011.12.002, 2012.

Dykoski, C. A., Edwards, R. L., Cheng, H., Yuan, D., Cai, Y., Zhang, M., Lin, Y., Qing, J., An, Z. and Revenaugh, J.: A high-resolution, absolute-dated Holocene and deglacial Asian monsoon record from Dongge Cave, China, Earth Planet. Sci. Lett., 233(1–2), 71–86, doi:10.1016/j.epsl.2005.01.036, 2005.

Enkin, R. J., Baker, J., Nourgaliev, D., Iassonov, P. and Hamilton, T. S.: Magnetic hysteresis parameters and Day plot analysis to characterize diagenetic alteration in gas hydrate-bearing sediments, J. Geophys. Res., 112(B06S90), 1–13, doi:10.1029/2006JB004638, 2007.

EPICA Community Members: One-to-one coupling of glacial climate variability in Greenland and Antarctica, Nature, 444(7116), 195–198, doi:10.1038/nature05301, 2006.

Favorite, F., Dodimead, A. J. and Nasu, K.: Oceanography of the Subarctic Pacific region, 1960-1971., 1976.

Galbraith, E. D., Jaccard, S. L., Pedersen, T. F., Sigman, D. M., Haug, G. H., Cook, M., Southon, J. R. and Francois, R.: Carbon dioxide release from the North Pacific abyss during the last deglaciation., Nature, 449(7164), 890–893, doi:10.1038/nature06227, 2007.

Gebhardt, H., Sarnthein, M., Grootes, P. M., Kiefer, T., Kuehn, H., Schmieder, F. and Röhl, U.: Paleonutrient and productivity records from the subarctic North Pacific for Pleistocene glacial terminations I to V, Paleoceanography, 23(4), doi:10.1029/2007PA001513, 2008.

Goldberg, E. L., Gorbarenko, S. A., Shaporenko, A. D., Bosin, A. A., Leskov, V. Y. and Chebykin, E.

Clim. Past Discuss., doi:10.5194/cp-2016-102, 2016
Manuscript under review for journal Clim. Past
Published: 1 November 2016

P. P.: Instability of last glacial climate from SRXFA data for bottom sediments in the Okhotsk Sea, Nucl. Instruments Methods Phys. Res. Sect. A Accel. Spectrometers, Detect. Assoc. Equip., 543(1), 284–287, doi:10.1016/j.nima.2005.01.242, 2005.

Gorbarenko, S. A.: Stable Isotope and Lithologic Evidence of Late-Glacial and Holocene Oceanography of the Northwestern Pacific and Its Marginal Seas, Quat. Res., 46(3), 230–250, doi:10.1006/qres.1996.0063, 1996.

Gorbarenko, S. A. and Goldberg, E. L.: Assessment of Variations of Primary Production in the Sea of Okhotsk, Bering Sea, and Northwestern Pacific over the Last Glaciation Maximum and Holocene, Dokl. Earth Sci., 405(9), 1380–1383, 2005.

Gorbarenko, S. A., Chekhovskaya, M. P. and Southon, J. R.: Detailed environmental changes of the Okhotsk Sea central part during last Glaciation Holocene, Oceanologia, 38(2), 305–308, 1998.

Gorbarenko, S. A., Leskov, V. Y., Artemova, A. V., Tiedemann, R., Biebow, N. and Nürnberg, D.: Ice Cover of the Sea of Okhotsk during the Last Glaciation and Holocene, Dokl. Earth Sci., 389(2), 208–211, 2003.

Gorbarenko, S. A., Basov, I. A., Chekhovskaya, M. P. P., Southon, J. R., Khusid, T. A. A. and Artemova, A. V.: Orbital and millennium scale environmental changes in the southern Bering Sea during the last glacial-Holocene: Geochemical and paleontological evidence, Deep Sea Res. Part II Top. Stud. Oceanogr., 52(16–18), 2174–2185, doi:10.1016/j.dsr2.2005.08.005, 2005.

Gorbarenko, S. A., Artemova, A. V., Goldberg, E. L. and Vasilenko, Y. P.: The response of the Okhotsk

Sea environment to the orbital-millennium global climate changes during the Last Glacial Maximum, deglaciation and Holocene, Glob. Planet. Change, 116, 76–90, doi:10.1016/j.gloplacha.2014.02.002, 2014.

Harada, N.: JAMSTEC cruise report: RV Mirai cruise MR06-04 LEG1., 2006.

Harris, P. G., Zhao, M., Rosell-Melé, A., Tiedemann, R., Sarnthein, M. and Maxwell, J. R.: Chlorin accumulation rate as a proxy for Quaternary marine primary productivity, Nature, 383(6595), 63–65, doi:10.1038/383063a0, 1996.

Hong, Y. T., Hong, B., Lin, Q. H., Shibata, Y., Zhu, Y. X., Leng, X. T. and Wang, Y.: Synchronous climate anomalies in the western North Pacific and North Atlantic regions during the last 14,000 years, Quat. Sci. Rev., 28(9–10), 840–849, doi:10.1016/j.quascirev.2008.11.011, 2009.

Hu, F. S., Kaufman, D., Yoneji, S., Nelson, D., Shemesh, A., Huang, Y., Tian, J., Bond, G. C., Clegg, B. and Brown, T. A.: Cyclic variation and solar forcing of Holocene climate in the Alaskan subarctic., Science, 301(5641), 1890–1893, doi:10.1126/science.1088568, 2003.

Jasonov, P. G., Nurgaliev, D. K., Burov, B. V. and Heller, F.: A modernized coercivity spectrometer, Geol. Carpathica, 49(3), 2254–225, 1998.

Johnsen, S. J., Clausen, H. B., Dansgaard, W., Fuhrer, K., Gundestrup, N., Hammer, C. U., Iversen, P., Jouzel, J., Stauffer, B. and Steffensen, J. P.: Irregular glacial interstadials recorded in a new Greenland ice core, Nature, 359(6393), 311–313, doi:10.1038/359311a0, 1992.

Keigwin, L. D.: Glacial-age hydrography of the far northwest Pacific Ocean, Paleoceanography, 13(4), 323–339, doi:10.1029/98PA00874, 1998.

Kienast, S. S. and McKay, J. L.: Sea surface temperature in the subartic Northeast Pacific reflect millennial-scale climate oscillations during the last 16 kyr, Geophys. Res. Lett., 28(8), 1563–1566, 2001.

Kuehn, H., Lembke-Jene, L., Gersonde, R., Esper, O., Lamy, F., Arz, H. W., Kuhn, G. and Tiedemann, R.: Laminated sediments in the Bering Sea reveal atmospheric teleconnections to Greenland climate on millennial to decadal timescales during the last deglaciation, Clim. Past, 10(6), 2215–2236, doi:10.5194/cp-10-2215-2014, 2014.

Lisitzin, A. P.: Sea-Ice and Iceberg Sedimentation in the Ocean, Springer, Berlin, Heidelberg., 2002.

Malakhov, M. I., Gorbarenko, S. A., Malakhova, G. Y., Harada, N., Vasilenko, Y. P., Bosin, A. A., Goldberg, E. L. and Derkachev, A. N.: Petromagnetic parameters of bottom sediments as indicators of the climatic and environmental changes in the central zone of the Sea of Okhotsk during the last 350 kyr, Russ. Geol. Geophys., 50(11), 973–982, doi:10.1016/j.rgg.2009.10.006, 2009.

Max, L., Riethdorf, J.-R., Tiedemann, R., Smirnova, M., Lembke-Jene, L., Fahl, K., Nürnberg, D., Matul, A. G. and Mollenhauer, G.: Sea surface temperature variability and sea-ice extent in the subarctic northwest Pacific during the past 15,000 years, Paleoceanography, 27(3), doi:10.1029/2012PA002292, 2012.

Max, L., Lembke-Jene, L., Riethdorf, J.-R., Tiedemann, R., Nürnberg, D., Kühn, H. and Mackensen, A.: Pulses of enhanced North Pacific Intermediate Water ventilation from the Okhotsk Sea and Bering

Sea during the last deglaciation, Clim. Past, 10(2), 591–605, doi:10.5194/cp-10-591-2014, 2014.

McManus, J. F., Francois, R., Gherardi, J.-M., Keigwin, L. D. and Brown-Leger, S.: Collapse and rapid resumption of Atlantic meridional circulation linked to deglacial climate changes., Nature, 428(6985), 834–837, doi:10.1038/nature02494, 2004.

Nagashima, K., Tada, R., Tani, A., Sun, Y., Isozaki, Y., Toyoda, S. and Hasegawa, H.: Millennial-scale oscillations of the westerly jet path during the last glacial period, J. Asian Earth Sci., 40(6), 1214–1220, doi:10.1016/j.jseaes.2010.08.010, 2011.

North Greenland Ice Core Project members: High-resolution record of Northern Hemisphere climate extending into the last interglacial period, Nature, 431(7005), 147–151, doi:10.1038/nature02805, 2004.

Nürnberg, D. and Tiedemann, R.: Environmental change in the Sea of Okhotsk during the last 1.1 million years, Paleoceanography, 19(4), PA4011, doi:10.1029/2004PA001023, 2004.

Okazaki, Y., Timmermann, A., Menviel, L., Harada, N., Abe-Ouchi, A., Chikamoto, M. O., Mouchet, A. and Asahi, H.: Deepwater formation in the North Pacific during the Last Glacial Termination., Science, 329(5988), 200–204, doi:10.1126/science.1190612, 2010.

Praetorius, S. K. and Mix, A. C.: Synchronization of North Pacific and Greenland climates preceded abrupt deglacial warming, Science, 345(6195), 444–448, doi:10.1126/science.1252000, 2014.

Rasmussen, S. O., Bigler, M., Blockley, S. P., Blunier, T., Buchardt, S. L., Clausen, H. B., Cvijanovic, I., Dahl-Jensen, D., Johnsen, S. J., Fischer, H., Gkinis, V., Guillevic, M., Hoek, W. Z., Lowe, J. J., Pedro, J. B., Popp, T., Seierstad, I. K., Steffensen, J. P., Svensson, A. M., Vallelonga, P., Vinther, B.

M., Walker, M. J. C., Wheatley, J. J. and Winstrup, M.: A stratigraphic framework for abrupt climatic changes during the Last Glacial period based on three synchronized Greenland ice-core records: refining and extending the INTIMATE event stratigraphy, Quat. Sci. Rev., 106, 14–28, doi:10.1016/j.quascirev.2014.09.007, 2014.

Reimer, P. J., Baillie, M. G. L., Bard, E., Beck, J. W., Bertrand, C. J. H., Blackwell, P. G., Buck, C. E., Burr, G. S., Cutler, K. B., Damon, P. E., Edwards, R. L., Fairbanks, R. G., Friedrich, M. and Guilderson, T. P.: IntCal04 terrestrial radiocarbon age calibration, 0–26 cal kyr BP, Radiocarbon, 46(3), 1029–1058, 2004.

Reimer, P. J., Baillie, M. G. L., Bard, E., Bayliss, A., Beck, J. W., Blackwell, P. G., Bronk Ramsey, C., Buck, C. E., Burr, G. S., Edwards, R. L., Friedrich, M., Grootes, P. M., Guilderson, T. P., Hajdas, I., Heaton, T. J., Hogg, A. G., Hughen, K. A., Kaiser, K. F., Kromer, B., McCormac, F. G., Manning, S. W., Reimer, R. W., Richards, D. A., Southon, J. R., Talamo, S., Turney, C. S. M., Van Der Plicht, J. and Weyhenmeyer, C. E.: IntCal09 and Marine09 radiocarbon age calibration curves, 0-50,000 yeats cal BP, Radiocarbon, 51(4), 1111–1150, doi:10.2458/rc.v51i4.3569, 2009.

Riethdorf, J.-R., Nürnberg, D., Max, L., Tiedemann, R., Gorbarenko, S. A. and Malakhov, M. I.: Millennial-scale variability of marine productivity and terrigenous matter supply in the western Bering Sea over the past 180 kyr, Clim. Past, 9(3), 1345–1373, doi:10.5194/cp-9-1345-2013, 2013.

Röhl, U. and Abrams, L. J.: High-resolution, downhole, and nondestructive core measurements from Sites 999 and 1001 in the Caribbean Sea: application to the Late Paleocene Thermal Maximum, in Proceedings of the Ocean Drilling Program, 165 Scientific Results, vol. 165, pp. 191–203, Ocean

Drilling Program., 2000.

Rohling, E. J., Liu, Q. S., Roberts, a. P., Stanford, J. D., Rasmussen, S. O., Langen, P. L. and Siddall, M.: Controls on the East Asian monsoon during the last glacial cycle, based on comparison between Hulu Cave and polar ice-core records, Quat. Sci. Rev., 28, 3291–3302, doi:10.1016/j.quascirev.2009.09.007, 2009.

Rossignol-Strick, M.: Mediterranean Quaternary sapropels, an immediate response of the African monsoon to variation of insolation, Palaeogeogr. Palaeoclimatol. Palaeoecol., 49(3–4), 237–263, doi:10.1016/0031-0182(85)90056-2, 1985.

Sakamoto, T., Ikehara, M., Aoki, K., Iijima, K., Kimura, N., Nakatsuka, T. and Wakatsuchi, M.: Ice-rafted debris (IRD)-based sea-ice expansion events during the past 100kyrs in the Okhotsk Sea, Deep Sea Res. Part II Top. Stud. Oceanogr., 52(16–18), 2275–2301, doi:10.1016/j.dsr2.2005.08.007, 2005.

Sarnthein, M., Kiefer, T., Grootes, P. M., Elderfield, H. and Erlenkeuser, H.: Warmings in the far northwestern Pacific promoted pre-Clovis immigration to America during Heinrich event 1, Geology, 34(3), 141–144, doi:10.1130/G22200.1, 2006.

Seierstad, I. K., Abbott, P. M., Bigler, M., Blunier, T., Bourne, A. J., Brook, E. J., Buchardt, S. L., Buizert, C., Clausen, H. B., Cook, E., Dahl-Jensen, D., Davies, S. M., Guillevic, M., Johnsen, S. J., Pedersen, D. S., Popp, T. J., Rasmussen, S. O., Severinghaus, J. P., Svensson, A. and Vinther, B. M.: Consistently dated records from the Greenland GRIP, GISP2 and NGRIP ice cores for the past 104 ka reveal regional millennial-scale δ18O gradients with possible Heinrich event imprint, Quat. Sci. Rev., 106, 29–46, doi:10.1016/j.quascirev.2014.10.032, 2014.

Seki, O., Ishiwatari, R. and Matsumoto, K.: Millennial climate oscillations in NE Pacific surface waters over the last 82 kyr: New evidence from alkenones, Geophys. Res. Lett., 29(23), 59-1-59–4, doi:10.1029/2002GL015200, 2002.

Seki, O., Ikehara, M., Kawamura, K., Nakatsuka, T., Ohnishi, K., Wakatsuchi, M., Narita, H. and Sakamoto, T.: Reconstruction of paleoproductivity in the Sea of Okhotsk over the last 30 kyr, Paleoceanography, 19(1), doi:10.1029/2002PA000808, 2004.

Serno, S., Winckler, G., Anderson, R. F., Maier, E., Ren, H., Gersonde, R. and Haug, G. H.: Comparing dust flux records from the Subarctic North Pacific and Greenland: Implications for atmospheric transport to Greenland and for the application of dust as a chronostratigraphic tool, Paleoceanography, 30(6), 583–600, doi:10.1002/2014PA002748, 2015.

Steffensen, J. P., Andersen, K. K., Bigler, M., Clausen, H. B., Dahl-Jensen, D., Fischer, H., Goto-Azuma, K., Hansson, M. E., Johnsen, S. J., Jouzel, J., Masson-Delmotte, V., Popp, T., Rasmussen, S. O., Röthlisberger, R., Ruth, U., Stauffer, B., Siggaard-Andersen, M.-L., Sveinbjörnsdóttir, A. E., Svensson, A. M. and White, J. W. C.: High-resolution Greenland ice core data show abrupt climate change happens in few years., Science, 321(5889), 680–684, doi:10.1126/science.1157707, 2008.

Stuiver, M. and Reimer, P. J.: Extended 14C Data Base and Revised Calib 3.0 14C Age Calibration Program, Radiocarbon, 35(1), 215–230, 1993.

Sun, Y., Clemens, S. C., Morrill, C., Lin, X., Wang, X. and An, Z.: Influence of Atlantic meridional overturning circulation on the East Asian winter monsoon, Nat. Geosci., 5(1), 46–49, doi:10.1038/ngeo1326, 2011.

Tauxe, L.: Sedimentary records of relative paleointensity of the geomagnetic field: Theory and practice, Rev. Geophys., 31(3), 319, doi:10.1029/93RG01771, 1993.

Walker, M. J. C., Berkelhammer, M., Björck, S., Cwynar, L. C., Fisher, D. A., Long, A. J., Lowe, J. J., Newnham, R. M., Rasmussen, S. O. and Weiss, H.: Formal subdivision of the Holocene Series/Epoch: a Discussion Paper by a Working Group of INTIMATE (Integration of ice-core, marine and terrestrial records) and the Subcommission on Quaternary Stratigraphy (International Commission on Stratigraphy), J. Quat. Sci., 27(7), 649–659, doi:10.1002/jqs.2565, 2012.

Wang, Y., Cheng, H., Edwards, R. L., An, Z., Wu, J., Shen, C.-C. and Dorale, J. A.: A high-resolution absolute-dated late Pleistocene Monsoon record from Hulu Cave, China., Science, 294(5550), 2345–8, doi:10.1126/science.1064618, 2001.

Wang, Y., Cheng, H., Edwards, R. L., He, Y., Kong, X., An, Z., Wu, J., Kelly, M. J., Dykoski, C. A. and Li, X.: The Holocene Asian monsoon: links to solar changes and North Atlantic climate., Science, 308(5723), 854–857, doi:10.1126/science.1106296, 2005.

Wang, Y., Cheng, H., Edwards, R. L., Kong, X., Shao, X., Chen, S., Wu, J., Jiang, X., Wang, X. and An, Z.: Millennial- and orbital-scale changes in the East Asian monsoon over the past 224,000 years., Nature, 451(7182), 1090–1093, doi:10.1038/nature06692, 2008.

Xue, F., Wang, H. and He, J.: Interannual Variability of Mascarene High and Australian High and Their

Influences on East Asian Summer Monsoon, J. Meteorol. Soc. Japan, 82(4), 1173–1186, doi:10.2151/jmsj.2004.1173, 2004.

Yu, J., Anderson, R. F., Jin, Z., Menviel, L., Zhang, F., Ryerson, F. J. and Rohling, E. J.: Deep South Atlantic carbonate chemistry and increased interocean deep water exchange during last deglaciation, Quat. Sci. Rev., 90, 80–89, doi:10.1016/j.quascirev.2014.02.018, 2014.

Yu, Y., Yang, T., Li, J., Liu, J., An, C., Liu, X., Fan, Z., Lu, Z., Li, Y. and Su, X.: Millennial-scale Holocene climate variability in the NW China drylands and links to the tropical Pacific and the North Atlantic, Palaeogeogr. Palaeoclimatol. Palaeoecol., 233(1–2), 149–162, doi:10.1016/j.palaeo.2005.09.008, 2006.

Yuan, D., Cheng, H., Edwards, R. L., Dykoski, C. A., Kelly, M. J., Zhang, M., Qing, J., Lin, Y., Wang, Y., Wu, J., Dorale, J. A., An, Z. and Cai, Y.: Timing, duration, and transitions of the last interglacial Asian monsoon., Science, 304(5670), 575–578, doi:10.1126/science.1091220, 2004.

Zijderveld, J. D. A.: A. C. demagnetization of rocks : analysis of results, in Methods in Palaeomagnetism, edited by D. W. Collinson, K. M. Creer, and S. K. Runcorn, pp. 254–286, Elsevier., 1964.

Clim. Past Discuss., doi:10.5194/cp-2016-102, 2016
Manuscript under review for journal Clim. Past
Published: 1 November 2016

Table 1. AMS ^{14}C data on monospecies planktonic foraminifera *N. pachyderma* sin. and benthic foraminifera *Epistominella pacifica* and *Uvigerina parvocastata* of core 41-2. All measured ^{14}C age data were corrected by NW Pacific surface water reservoir ages of 900 years (Max et al., 2012). In case of using benthic foraminifera for dating we accept difference in coeval benthic-planktic foraminifera ages equals to 1400 years for depth water 1900 m, based on the unpublished and total regional results of Max et al. (2014). All radiocarbon ages were converted into calibrated 1-sigma calendar age using the calibration program CALIB REV 7.0.1 (Stuiver and Reimer, 1993) with the Marine13 calibration curve (Reimer et al., 2013).

#	Lab. code	core depth cm	foraminifera species	14C-age year	Err.1 sigma year	calendar age, years	calendar age, ka
1	YAUT-021713	120	*E. pacifica*	10078	47	9121	9.121
2	YAUT-021714	127.5	*E. pacifica*	10340	42	9445	9.445
3	UCIAMS-148095	298	*N. pachyd.*	13160	50	14393	14.393
4	UCIAMS-148096	156	*Uv. parvoc.*	11135	45	10600	10.60
5	UCIAMS-148098	306	*Uv. parvoc.*	14185	35	16,016	14.616

Clim. Past Discuss., doi:10.5194/cp-2016-102, 2016
Manuscript under review for journal Clim. Past
Published: 1 November 2016

Climate of the Past Discussions

Table 2.The key time points of core 41-2 based on the available AMS ^{14}C data of core 41-2, depths correlated with AMS ^{14}C data of core 12KL plus depth correlation of the productivity cycles with highly resolved, absolutely dated E Asia monsoon related CsIs (Wang et al., 2008).

Depth cm	AMS ^{14}C core 41-2 (cal. kyr BP)	AMS ^{14}C data (ka)/ depth of core 12KL. cm	correlation with ages of China sub-Interstadial	calendar age ka
120	9.12			9.12
127.5	9.45			
126		9.51/210		9.51
156	10.6			
159		11.08/295		11.08
167		11.31/340		11.31
251		13.38/508		13.38
273		13.79/550		13.79
298	14.39			
303		14.42/611		14.42
306	14.61			
337			15.42	15.42
347		15.9(15.55)/695		
357			16.51	16.51
382			17.56	17.56
393			18.12	18.12
402		18.6/821		
405			18.8	18.8
431		19.54/876		
438			19.8	19.8

735 Figures

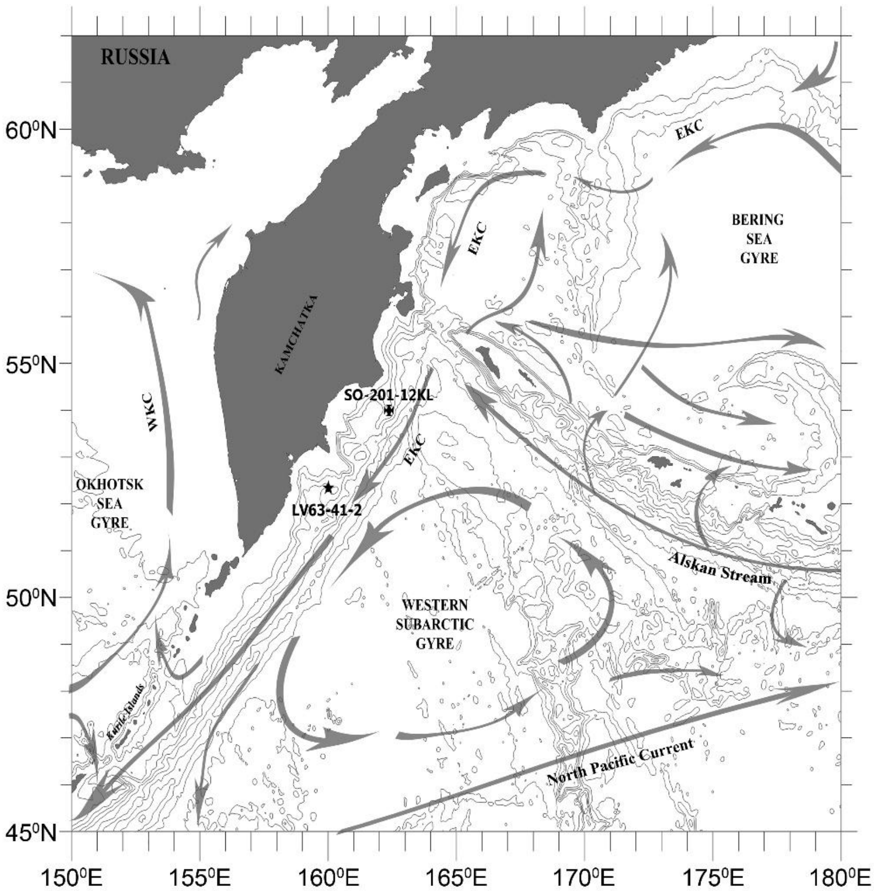

Fig. 1. Bathymetry, surface water currents and location of the cores 41-2 (star) and 12KL (cross) (Max et al., 2012) in the North Pacific. Surface currents as in (Favorite et al., 1976) with modifications. EKC – East Kamchatka Current, WKC – West Kamchatka Current.

740

Clim. Past Discuss., doi:10.5194/cp-2016-102, 2016
Manuscript under review for journal Clim. Past
Published: 1 November 2016

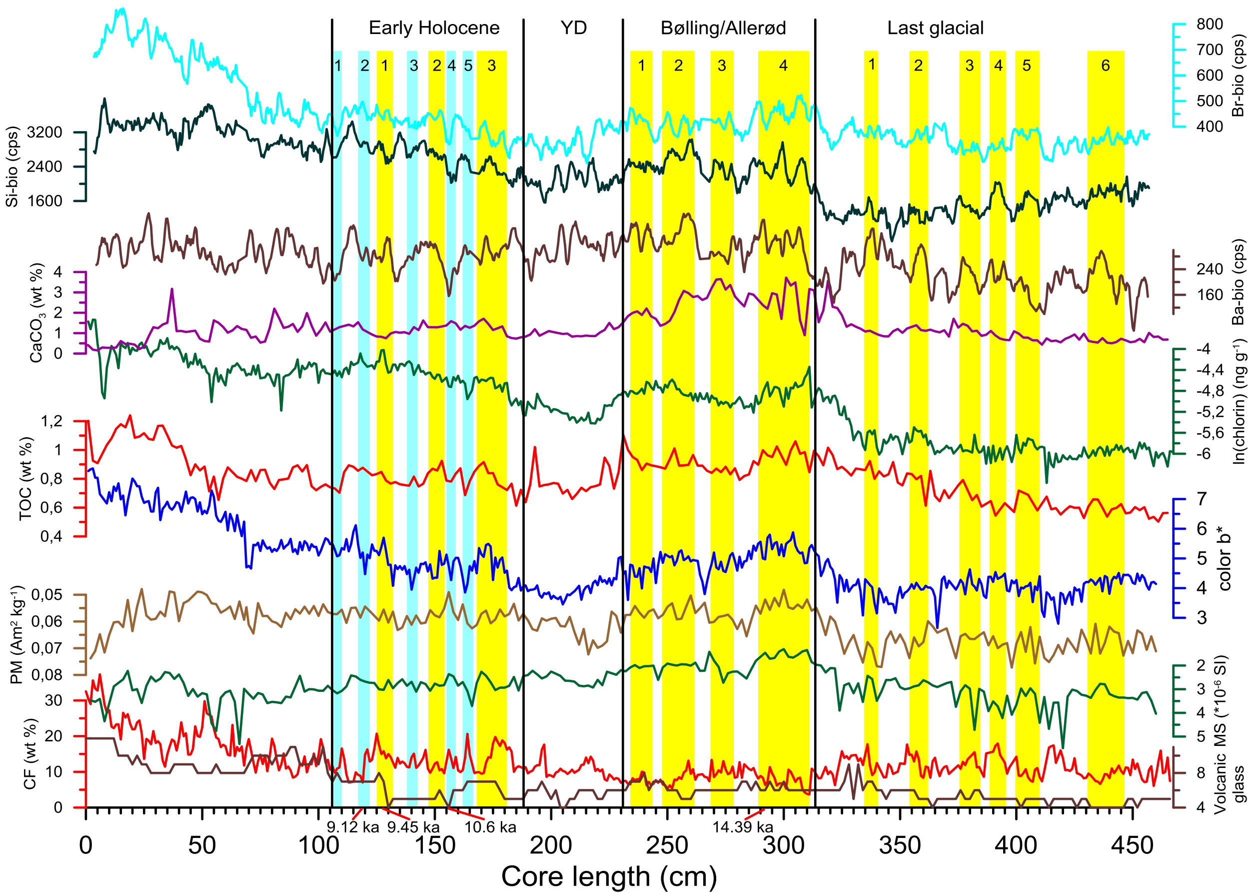

Fig. 2. Records (from bottom to top) of the weight percentages of the CF, share of volcanic grains in the sediment fraction more 150 µm, magnetic susceptibility (MS), paramagnetic magnetization (PM), color b*; TOC, Chlorin, $CaCO_3$, Ba-bio, Si-bio (opal) and Br-bio content versus core 41-2 depth. Preliminary boundaries of B/A warming, YD cooling and Holocene are shown according to total reguliarities of productivity variability in the NW Pacific, the Sea of Okhotsk and Bering Sea (Galbraith et al., 2007; Gorbarenko, 1996; Gorbarenko and Goldberg, 2005; Keigwin, 1998; Seki et al., 2004) and AMS ^{14}C data (calendar ka) shown at the base.Yellow bars depict the centennial-millenial increased productivity/environmental ameloiration events according to most productivity proxies and decreases in

Clim. Past Discuss., doi:10.5194/cp-2016-102, 2016
Manuscript under review for journal Clim. Past
Published: 1 November 2016

PM. Blue bars depict the centennial-millennial decreased productivity/environmental cooling events during EH.

Clim. Past Discuss., doi:10.5194/cp-2016-102, 2016
Manuscript under review for journal Clim. Past
Published: 1 November 2016

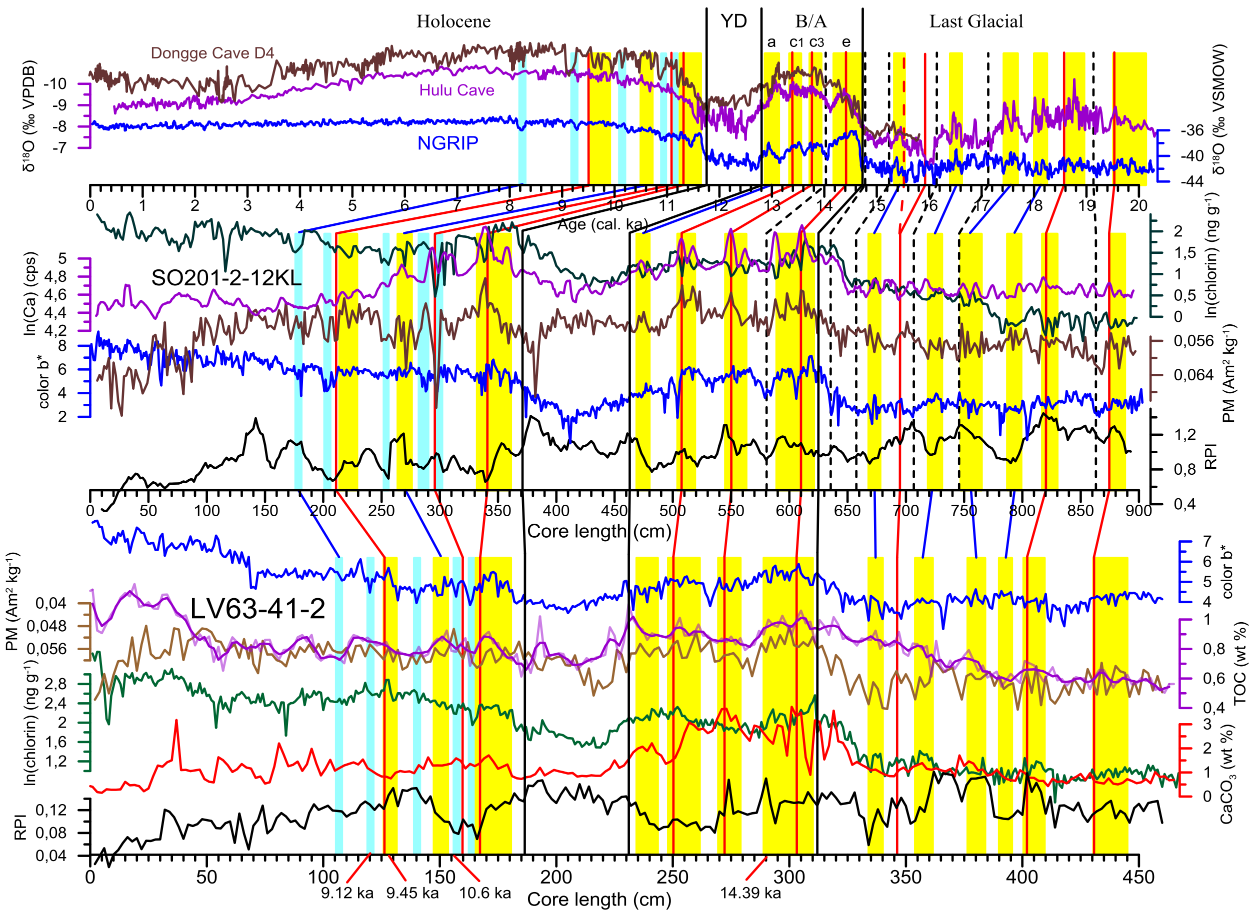

Fig. 3. Correlation of the productivity cycles in the cores 41-2 (low panel) and 12KL (middle panel) versus depth with sub-interstadials of the δ^{18}O calcite of Chinese stalagmites (Dykoski et al., 2005; Wang et al., 2008) (upper panel) and key time points of core 41-2 shown by red lines. Productivity cycles for cores 41-2 based on suite of productivity proxies and PM records (Fig. 2) and 12KL (Ca, chlorin and color b* and PM records) were correlated according to sychronously changes in productivity proxies, paramagnetic magnetization, magnetic relative paleomagnetic intensity (RPI) and ^{14}C AMS data of the both cores. According to correlation of the productivity cycles and curves of RPI, red lines related with ^{14}C AMS data of core 12KL (middle panel) were projected into corresponded

depths of core 41-2 (bottom panel). Color b* and Ca content, AMS ^{14}C data of core 12KL and its depth-age correlation with the Greenland NGRIP ice core were introduced from site http://dx.doi.org/10.1594/PANGAEA.830222. Blue lines correlate the productivity cycles of cores 41-2 and 12KL with relative Chinese sub-interstadials of the $\delta^{18}O$ calcite of Chinese stalagmites (Dykoski et al., 2005; Wang et al., 2008) during LGM- EH in consistence with their age models.

Clim. Past Discuss., doi:10.5194/cp-2016-102, 2016
Manuscript under review for journal Clim. Past
Published: 1 November 2016

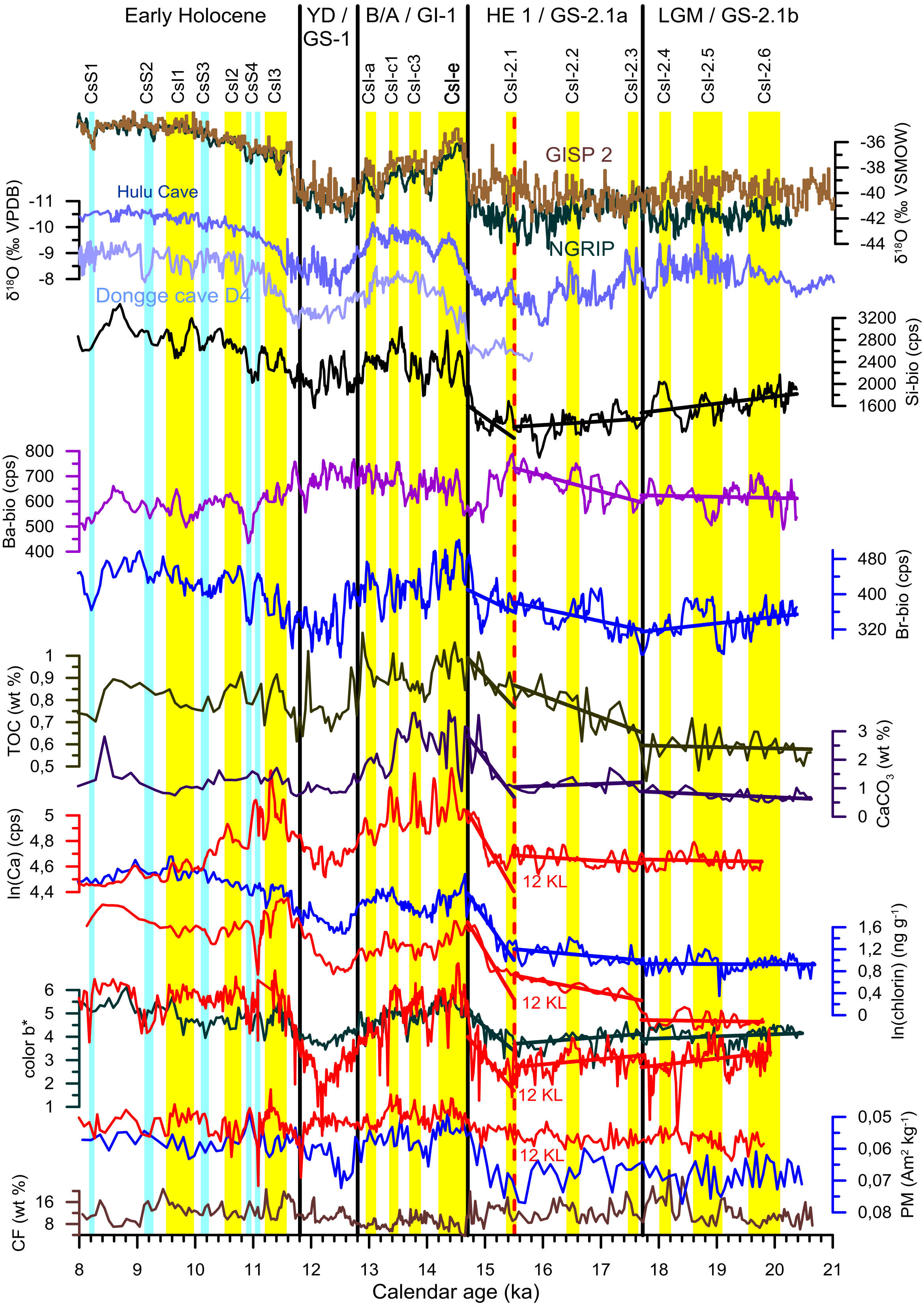

Clim. Past Discuss., doi:10.5194/cp-2016-102, 2016
Manuscript under review for journal Clim. Past
Published: 1 November 2016

Fig. 4. High resolution variability of the productivity and lithologic proxies in NW Pacific (off Kamchatka) over the 21-8 ka ago period. CF percentages, paramagnetic magnetization and color b*, chlorin , $CaCO_3$, TOC, Br-bio, Ba-bio and Si-bio (analog of biogenic opal) content determined in cores 41-2 and 12KL (red lines) are shown from bottom to top. The NW Pacific centennial-millennial productivity cycles characterized by increase in most productivity proxies are clearly associated with the abrupt summer EAM intensification revealed in Chinese cave stalagmites called as sub Interstadial and less pronounced with short term events in the Greenland ice cores $\delta^{18}O$ records. Linear lines show trends of the siliceous and carbonaceous related productivity indices over LGM and HE 1.

Clim. Past Discuss., doi:10.5194/cp-2016-102, 2016
Manuscript under review for journal Clim. Past
Published: 1 November 2016

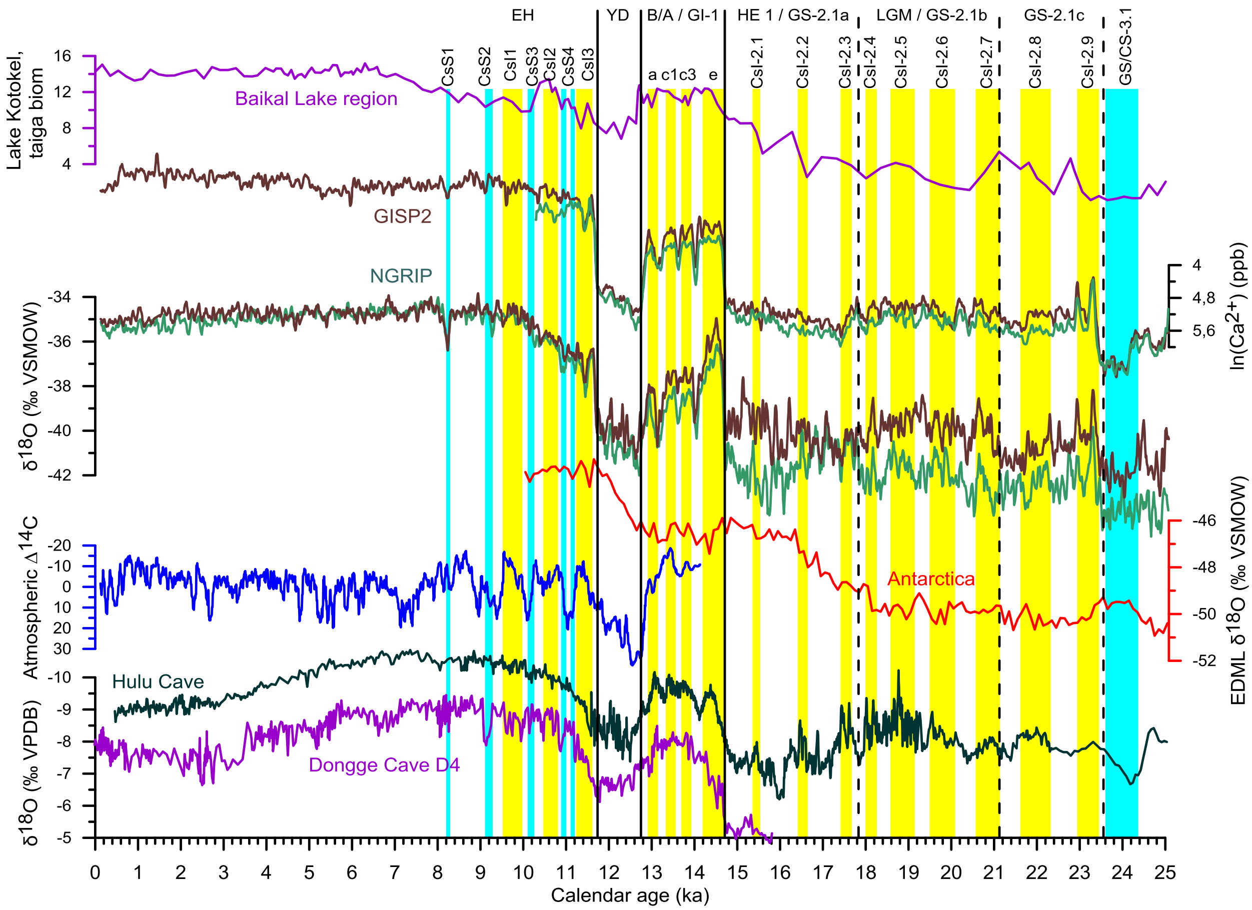

Fig. 5. Compilation on N-S hemisphere milestone climate records, solar activity, NW Pacific productivity cycles and Southern Siberia environment during the last 25 ka. From bottom to top: absolutely dated $\delta^{18}O$ calcite of Chinese cave stalagmites (Dykoski et al., 2005; Wang et al., 2008) characterized EAM activity; the residual atmospheric $\Delta^{14}C$ record of around 2000-year moving average (Reimer et al., 2004) indicated solar irradiance variability; oxygen isotope EDML records after methane synchronization with North Greenland ice core (EPICA Community Members, 2006); the $\delta^{18}O$ and Ca^{2+} records in the Greenland NGRIP and GISP 2 ice core indicated air temperature and dust variability on GICC05 age scale (Rasmussen et al., 2014), and pollen reconstructed Southern Siberia environment

Clim. Past Discuss., doi:10.5194/cp-2016-102, 2016
Manuscript under review for journal Clim. Past
Published: 1 November 2016

changes (Lake Kotokel, Lake Baikal region) (Bezrukova et al., 2011). The vertical yellow bands trace the centennial-millennial NW Pacific productivity cycles with increased productivity, blue bars GS/CS-3.1 (HE 2) and Early Holocene short term coolings. NW Pacific centennial-millennial productivity cycles are accompanied by interstadial and sub-interstadial intensification of the summer EAM over 25-8 ka ago and increase of solar irradiance during B/A and EH short term warmings. Their correlation with short term increased Greenland temperature (NGRIP ice core) and a decreased Antarctic temperature are less pronounced but seem to be marked as well.

Clim. Past Discuss., doi:10.5194/cp-2016-102, 2016
Manuscript under review for journal Clim. Past
Published: 1 November 2016

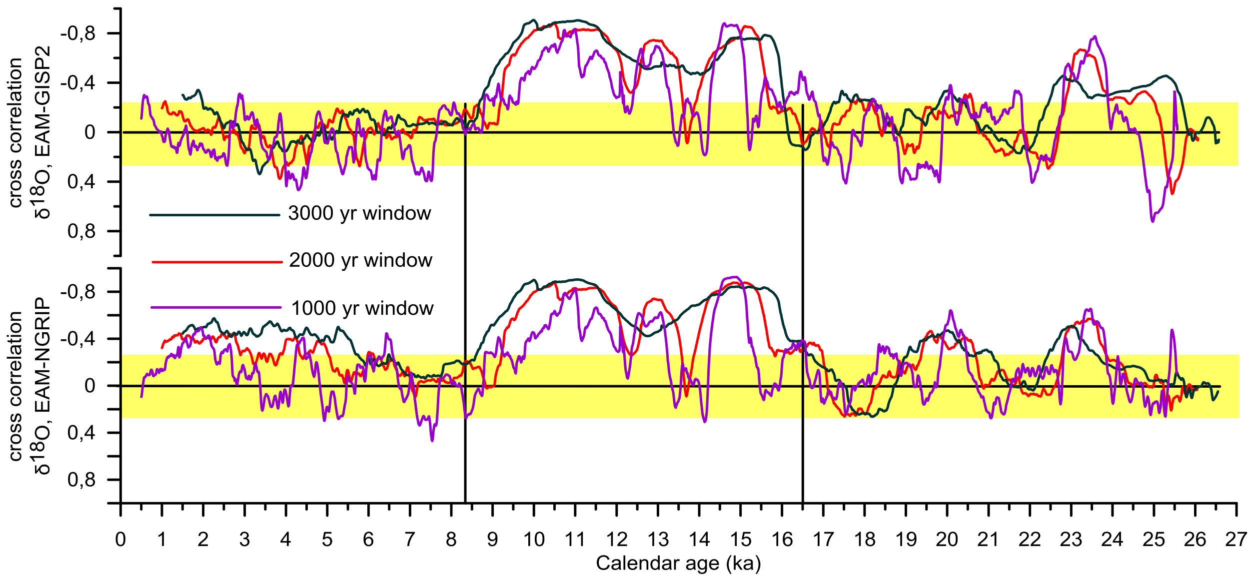

Fig. 6. Cross correlation of the EAM and Greenland climate variability calculated by correlation of $\delta^{18}O$ values of the calcite of Chinese stalagmites (Wang et al., 2008) with ones of the NGRIP (lower panel) and with ones of the GISP 2 (upper panel) ice cores (Rasmussen et al., 2014) by moving windows at 1000 years (purple lines), 2000 years (red lines) and 3000 years (green lines) over the last 25 ka. Yellow bars show areas with insignificant cross correlation ranging between +0.25 and -0.25. Cross correlation between the EAM and Greenland by moving window 3000 years is negative during period of 16.5-9.0 ka and insignificant or weakly negative during earlier and later periods of 25-16.5 ka and of 9.0-0 ka BP confirmed the EAM and the Greenland synchronicity.